

Stretchable optical waveguides

Jeroen Missinne*, Sandeep Kalathimekkad, Bram Van Hoe,
Erwin Bosman, Jan Vanfleteren, and Geert Van Steenberge

Centre for Microsystems Technology (CMST), imec and Ghent University,
Technologiepark 914a, 9052 Gent, Belgium

*jeroen.missinne@elis.ugent.be

Abstract: We introduce the concept of mechanically stretchable optical waveguides. The technology to fabricate these waveguides is based on a cost-efficient replication method, employing commercially available polydimethylsiloxane (PDMS) materials. Furthermore, VCSELs ($\lambda = 850$ nm) and photodiodes, embedded in a flexible package, were integrated with the waveguides to obtain a truly bendable, stretchable and mechanically deformable optical link. Since these sources and detectors were integrated, it was possible to determine the influence of bending and stretching on the waveguide performance.

© 2014 Optical Society of America

OCIS codes: (250.0250) Optoelectronics; (250.5460) Polymer waveguides; (230.0230) Optical devices; (230.3120) Integrated optics devices.

References and links

1. V. Lumelsky, M. Shur, and S. Wagner, "Sensitive Skin Workshop, Arlington, Virginia," NSF, DARPA Sensitive Skin Workshop Report pp. 1–129 (1999).
2. S. Cheng and Z. Wu, "A microfluidic, reversibly stretchable, large-area wireless strain sensor," *Adv. Funct. Mater.* **21**, 2282–2290 (2011).
3. Nokia, "The Morph Concept," <https://research.nokia.com/morph> (accessed 2013).
4. R. Verplancke, F. Bossuyt, D. Cuypers, and J. Vanfleteren, "Thin-film stretchable electronics technology based on meandering interconnections: fabrication and mechanical performance," *J. Micromech. Microeng.* **22**, 015002 (2012).
5. F. Bossuyt, T. Vervust, and J. Vanfleteren, "Stretchable electronics technology for large area applications: fabrication and mechanical characterization," *IEEE Trans. Comp. Pack. Man.* **3**, 229–235 (2013).
6. T. Li, Z. Huang, Z. Suo, S. P. Lacour, and S. Wagner, "Stretchability of thin metal films on elastomer substrates," *Appl. Phys. Lett.* **85**, 3435–3437 (2004).
7. J. A. Rogers, T. Someya, and Y. Huang, "Materials and mechanics for stretchable electronics," *Science* **327**, 1603–1607 (2010).
8. T. Sekitani, Y. Noguchi, K. Hata, T. Fukushima, T. Aida, and T. Someya, "A rubberlike stretchable active matrix using elastic conductors," *Science* **321**, 1468–1472 (2008).
9. D. Pham, H. Subbaraman, M. Chen, X. Xu, and R. Chen, "Self-aligned carbon nanotube thin-film transistors on flexible substrates with novel source-drain contact and multilayer metal interconnection," *IEEE Trans. Nanotechnol.* **11**, 44–50 (2012).
10. D.-H. Kim, J.-H. Ahn, W. M. Choi, H.-S. Kim, T.-H. Kim, J. Song, Y. Y. Huang, Z. Liu, C. Lu, and J. A. Rogers, "Stretchable and foldable silicon integrated circuits," *Science* **320**, 507–511 (2008).
11. B. Van Hoe, G. Van Steenberge, E. Bosman, J. Missinne, T. Geernaert, F. Berghmans, D. Webb, and P. Van Daele, "Optical fiber sensors embedded in flexible polymer foils," in *Optical Sensing and Detection*, F. Berghmans, A. G. Mignani, and C. A. van Hoof, eds., Proc. SPIE **7726**, 72603–72603–10 (2010).
12. J. Garra, T. Long, J. Currie, T. Schneider, R. White, and M. Paranjape, "Dry etching of polydimethylsiloxane for microfluidic systems," *J. Vac. Sci. Technol. A* **20**, 975–982 (2002).
13. M. Schuettler, C. Henle, J. Ordonez, G. Suaning, N. Lovell, and T. Stieglitz, "Patterning of silicone rubber for micro-electrode array fabrication," in *Proceedings of International IEEE/EMBS Conference on Neural Engineering* (Institute of Electrical and Electronics Engineers, New York, 1988), pp. 53–56.
14. D. Szmigiel, K. Domanski, P. Prokaryn, and P. Grabiec, "Deep etching of biocompatible silicone rubber," *Microelectron. Eng.* **83**, 1178–1181 (2006).

15. S. J. Hwang, D. J. Oh, P. G. Jung, S. M. Lee, J. S. Go, J.-H. Kim, K.-Y. Hwang, and J. S. Ko, "Dry etching of polydimethylsiloxane using microwave plasma," *J. Micromech. Microeng.* **19**, 095010 (2009).
16. B. A. Fogarty, K. E. Heppert, T. J. Cory, K. R. Hulbutta, R. S. Martin, and S. M. Lunte, "Rapid fabrication of poly(dimethylsiloxane)-based microchip capillary electrophoresis devices using CO₂ laser ablation," *Analyst* **130**, 924–930 (2005).
17. Y. Xia and G. M. Whitesides, "Soft lithography," *Annu. Rev. Mater. Sci.* **28**, 153–184 (1998).
18. D. A. Chang-Yen, R. K. Eich, and B. K. Gale, "A monolithic PDMS waveguide system fabricated using soft-lithography techniques," *J. Lightwave Technol.* **23**, 2088 (2005).
19. J. S. Kee, D. P. Poenar, P. Neuzil, and L. Yobas, "Monolithic integration of poly(dimethylsiloxane) waveguides and microfluidics for on-chip absorbance measurements," *Sensor. Actuat. B-Chem.* **134**, 532–538 (2008).
20. S. Kopetz, D. Cai, E. Rabe, and A. Neyer, "PDMS-based optical waveguide layer for integration in electrical-optical circuit boards," *AEU-Int. J. Electron. Commun.* **61**, 163–167 (2007).
21. K. S. Ryu, X. Wang, K. Shaikh, and C. Liu, "A method for precision patterning of silicone elastomer and its applications," *J. Microelectromech. Syst.* **13**, 568–575 (2004).
22. J. S. Kee and D. P. Poenar and P. Neuzil and L. Yobas, "Design and fabrication of poly(dimethylsiloxane) single-mode rib waveguide," *Opt. Express* **17**, 11739–11746 (2009).
23. V. Lien, Y. Berdichevsky, and Y.-H. Lo, "A prealigned process of integrating optical waveguides with microfluidic devices," *IEEE Photon. Technol. Lett.* **16**, 1525–1527 (2004).
24. V. Lien, K. Zhao, Y. Berdichevsky, and Y.-H. Lo, "High-sensitivity cytometric detection using fluidic-photonics integrated circuits with array waveguides," *IEEE J. Sel. Top. Quantum Electron.* **11**, 827–834 (2005).
25. N. Bamiedakis, R. Penty, and I. White, "Compact multimode polymer waveguide bends for board-level optical interconnects," *J. Lightwave Technol.* **31**, 2370–2375 (2013).
26. B. Riegler and R. Thomaier, "Index matching silicone for optoelectronic applications," in *New Developments in Optomechanics*, A. E. Hatheway, eds., Proc. SPIE **6665**, 666508–666508–8 (2007).
27. S. Bhattacharya, A. Datta, J. Berg, and S. Gangopadhyay, "Studies on surface wettability of poly(dimethyl) siloxane (PDMS) and glass under oxygen-plasma treatment and correlation with bond strength," *J. Microelectromech. Syst.* **14**, 590–597 (2005).
28. B. Van Hoe, E. Bosman, J. Missinne, S. Kalathimekkad, G. Van Steenberge, and P. Van Daele, "Novel coupling and packaging approaches for optical interconnects," in *Optoelectronic Interconnects XII*, A. L. Glebov and R. T. Chen, eds., Proc. SPIE **8267**, 82670T–82670T–11 (2012).

1. Introduction

Stretchable material technologies have enabled an emerging range of applications that are impossible to achieve using conventional rigid or flexible technologies. Examples can be found in diverse application domains such as robotics and automation, health care and biomedical technologies, and consumer electronics. The ability to deform a functional substrate so that it can be wrapped around a curved or moving surface, allows for example creating an artificial (robot) skin [1], wearable on-body sensing systems [2], or even monitoring moving machine parts or electronic systems that conform to their environment [3].

A considerable amount of research has been performed on stretchable electronic systems in which, for example, non-stretchable islands are embedded in a stretchable material such as polydimethylsiloxane (PDMS), and joined with electrical interconnections. To make these interconnections mechanically stretchable, 2 approaches have been adopted. In a first approach, traditional conductors such as copper, gold or silicon are patterned as spring-like structures instead of straight lines [4–7]. In a second approach, an electrically conductive stretchable material itself is used to create the interconnections [8]. Furthermore, not only the interconnections, but also electronic components themselves can be made flexible [9] or stretchable [10].

Nowadays, more and more (sensing) systems are implemented using optical instead of electrical technologies and it can therefore be expected that in addition to stretchable electrical interconnections, there will also be a need for stretchable optical interconnections. To make optical interconnections stretchable, 2 analogous approaches can be defined, i.e. using either meandering, or straight optical waveguiding structures. Related to the first approach, meandering silica optical fibers have previously been embedded in a PDMS material, so that the final assembly becomes stretchable [11]. For shorter interconnection lengths, however, the use of planar waveguides is more convenient. Most of the traditional optical waveguide materials (for

example glass, semiconductors or polymers) are rigid or in the best case flexible and would similarly require to pattern them in a meandering fashion and embed them in a stretchable host material to make stretchable interconnections. This approach is much more challenging compared to the electrical case, both from a design and technological point of view. Therefore, this paper introduces the concept of straight stretchable optical waveguides fabricated using less conventional, but highly stretchable and optically transparent PDMS materials.

The majority of available PDMS materials is not suited for traditional photolithographic pattern definition. Although patterning of PDMS using wet chemical etching [12, 13], reactive ion etching [12, 14, 15] and laser ablation [16] has been reported, mainly replication based microfabrication techniques are used, and are generally referred to as ‘soft lithography’ [17]. Specifically for fabricating waveguides in PDMS, several approaches have been reported differing in applied patterning technologies and methods to obtain the refractive index contrast required for waveguiding.

A first approach to introduce an index contrast is to use a single material, for example Sylgard®184 (Dow Corning) but differing the mixing ratios of prepolymer and curing agent or the (thermal) curing conditions [18]. Alternatively, in [19], Sylgard®184 was mixed with a silicone oil (200®Fluid, Dow Corning) to increase the refractive index. Furthermore, PDMS can be chemically modified for example by incorporating phenyl groups in the side chains of the PDMS-backbone [20] in order to obtain a new material with a different refractive index. It is clear that all these approaches require precise tuning of parameters or proprietary material development. However, recently, many types of optically transparent PDMS materials with a range of different refractive indexes have become commercially available and can directly be applied. This allows selecting 2 materials with a precise refractive index difference for the core and cladding, depending on the waveguide design.

To pattern waveguides in PDMS, a widely adopted approach is to precisely fill microchannels using a razor blade or squeegee [18, 20–22]. Hereby, the challenge is to remove the excess material to avoid a residual layer between the different waveguide cores since this may cause cross-talk between neighboring channels. As an alternative, closed microchannels can be patterned in cladding material and subsequently capillary filled with another material that forms the core of the waveguide [23, 24].

In this paper, we introduce the concept of stretchable optical interconnections based on multimode PDMS waveguides. To adopt a widely applicable and cost-efficient technology, only commercially available materials are used and the waveguides are patterned using a replication technology based on the capillary filling of PDMS microchannels. This previously reported method was modified to obtain freestanding PDMS waveguides with integrated optoelectronic sources and detectors, resulting in a truly stretchable and complete optical link. By having the sources and detectors integrated, it was also possible to study the optical link behavior under mechanical deformation.

2. Fabrication methods

2.1. Waveguide design and materials

The waveguides consist of 6 cm long multimode channels with a cross-section of $50\ \mu\text{m} \times 50\ \mu\text{m}$. These are typical dimensions for multimode waveguides providing 1dB alignment tolerances larger than $\pm 10\ \mu\text{m}$ for in- and outcoupling [25]. To maximize the light confinement, the refractive index contrast between cladding and core was chosen as large as possible within the limits of available materials. Therefore, Sylgard®184 (Dow Corning, refractive index $n_{\text{cladding}} = 1.41$) was used as cladding and LS-6257 (Nusil, refractive index $n_{\text{core}} = 1.57$) was used as core material, resulting in a waveguide numerical aperture (NA) of

$\sqrt{n_{core}^2 - n_{cladding}^2} = 0.69$. The higher this value, the smaller bending radii are possible, which is important when designing deformable waveguides. As operating wavelength, 850 nm was selected, for which optoelectronic sources and detectors are available and the intrinsic losses of both materials are low. According to the product specifications, the intrinsic loss of the LS-6257 material is below 0.05 dB/cm [26] and based on internal experience, Sylgard®184 is expected to exhibit a similar intrinsic loss value.

2.2. Waveguide fabrication

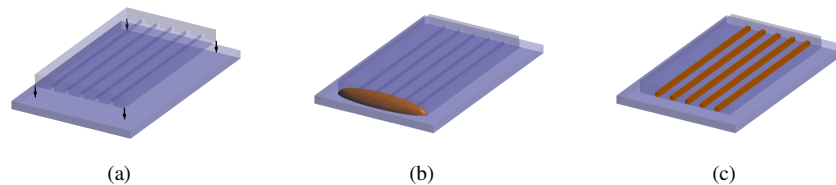


Fig. 1. Simplified concept of the PDMS waveguide fabrication process based on a capillary filling technique: (a) Bonding of 2 PDMS layers forming covered channels, (b) Applying a drop of liquid core material at the inlet, (c) Curing the core material once the channels are filled.

The multimode waveguides were patterned using a replication technique, see Fig. 1. First, a master mold was fabricated by defining $50\ \mu\text{m} \times 50\ \mu\text{m}$ SU-8 ribs on a $250\ \mu\text{m}$ pitch using UV lithography on a silicon wafer. This master mold was over-coated with Sylgard®184 (Dow Corning), which was subsequently thermally cured (15 minutes at 100°C on a hotplate) and then released. This layer forms the bottom cladding of the waveguides. Another, temporary, $10\ \text{cm} \times 10\ \text{cm}$ glass substrate was covered with a spin-coated release layer of a 4% weight/volume polyvinyl alcohol solution in water (PVA, molecular weight between 31k and 50k, Sigma Aldrich). Then, a $25\ \mu\text{m}$ thick layer of Sylgard®184 was spin-coated onto this release layer, forming the top cladding of the waveguides. Both the patterned and unpatterned cladding substrates were plasma treated (Diener Pico, 0.8 mbar, 24 s, 190 W 40 kHz generator, gas used: air) and subsequently brought in contact to form channels. This plasma treatment creates silanol groups on the surface forming an irreversible Si-O-Si bond upon contact [27]. Then, a drop of another type of PDMS, LS-6257 (Nusil) was applied at the inlet of the channels, filling them using the capillary action. After complete filling of the channels, the material was thermally cured for 14 hours in an oven at 80°C , realizing the waveguides. Finally, the waveguide substrate was immersed in deionized water for 1 hour to dissolve the PVA layer and obtain the freestanding, stretchable waveguides.

To interface the waveguides and create end-faces, a precise cut was made perpendicular to the waveguides using a thin razor blade. A photo of such a cut is shown in Fig. 2 also illustrating the dimensions of the waveguides. Due to the softness of the PDMS materials (Durometer, Shore A 50 for Sylgard®184 and Shore A 40 for LS-6257), polishing of the waveguide end-faces is difficult and was therefore not applied.



Fig. 2. Razor blade cross-section of the PDMS waveguides fabricated using capillary filling.

2.3. Integration of light sources and detectors

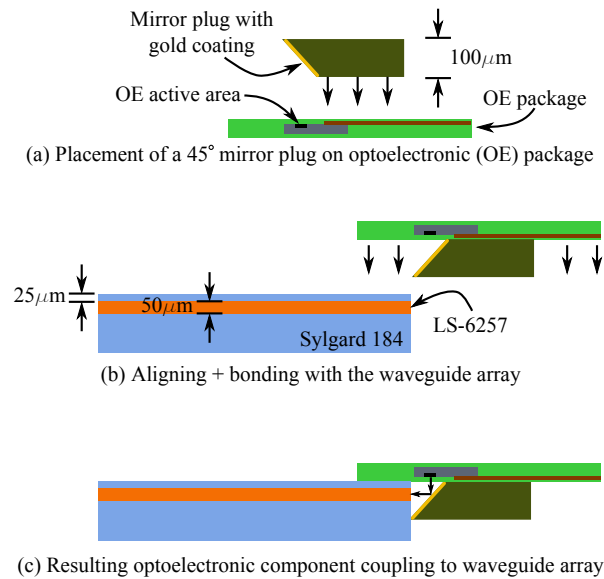


Fig. 3. Fabrication steps for integrating optoelectronic components with stretchable waveguides; the procedure is identical for integrating VCSELs or photodiodes.

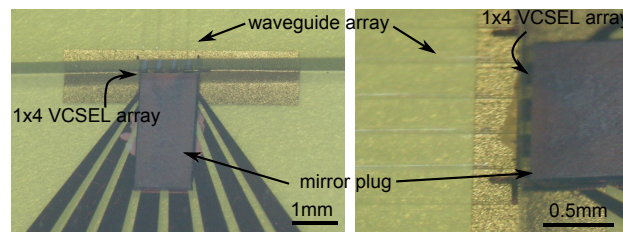


Fig. 4. Embedded 1x4 VCSEL array coupled to 4 PDMS waveguides using the process shown in Fig. 3. The optoelectronic component is covered by the mirror plug and can therefore not be seen.

In order to characterize waveguides, interfacing with sources and detectors is needed. Usually, waveguides are characterized using actively aligned optical fibers at the input and output. However, for investigating the behavior of waveguides under mechanical bending, and especially stretching, this method becomes difficult, if not impossible. Therefore, a process was developed to integrate light sources and detectors with the waveguides [28], as illustrated in Fig. 3.

As a starting point for this process, the technology for embedding thinned, bare die VCSELs (850 nm, multimode 1x4 array, ULM Photonics ULM850-05-TT) and photodiodes (GaAs, 100 μm circular active area, 1x4 array, Enablence, PDCA04-100-GS) in 40 μm thick, flexible polyimide foils was used. A 100 μm thick 45° deflecting micro mirror plug (material: polyimide) with a 120 nm evaporated gold coating was aligned with the active areas of these embedded optoelectronic components using a Dr. Tresky flip-chip bonder and subsequently glued using XS8455-48 adhesive (Namics corporation). The divergence angle of the VCSEL

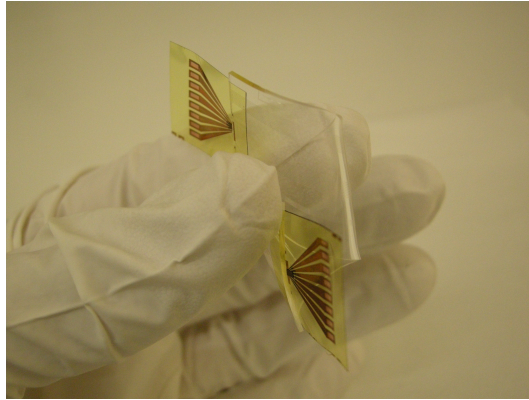


Fig. 5. Photo of the complete stretchable optical link including embedded VCSELs and photodiodes integrated with PDMS waveguides.

(20° , full width $1/e^2$ at 5 mA driving current) is small enough and the active area of the photodiode is large enough to ensure efficient coupling to the $50\ \mu\text{m} \times 50\ \mu\text{m}$ waveguides after bridging the $100\ \mu\text{m}$ distance between active area, mirror plug and waveguide end-face.

Subsequently, this complete assembly was aligned and bonded with the PDMS-based optical waveguides. To ensure proper vertical alignment, the waveguides top cladding thickness was precisely controlled to $25\ \mu\text{m}$, while the lateral positioning was performed using marks on the polyimide substrate which were aligned to the waveguides using a modified mask aligner. For achieving precise bonding of the PDMS and the polyimide substrate, a ‘dry bonding’ technique was used. Therefore, a $50\ \text{nm}$ SiO_2 layer was coated on the polyimide substrate, and then the PDMS and the coated polyimide substrate were plasma treated (Diener Pico, 0.8 mbar, 24 s, 190 W 40 kHz generator, gas used: air) creating silanol groups on both substrates. When the silanol groups on these 2 treated surfaces are brought into contact, an irreversible Si-O-Si bond is formed [27].

After this process, a small drop of Sylgard®184 was dispensed to fill the air gap between the waveguide end-faces and the mirror plug, acting as index matching material. This drop of material was left curing at room temperature in order not to induce thermal stress which may shift the components and affect the optical alignment.

Figure 4 shows a microscope view of an embedded optoelectronic component (1x4 VCSEL array) which is optically coupled to 4 PDMS waveguides using the 45° deflecting micro mirror plug and Fig. 5 shows a photo of the complete stretchable link including integrated light sources and detectors.

3. Characterization methods

The stretchable waveguides were characterized in terms of propagation losses, bending losses, stretching losses and reliability.

In this paper, the total link loss was determined, i.e. from VCSEL, coupled into a 6 cm, $50\ \mu\text{m} \times 50\ \mu\text{m}$ waveguide and coupled out to the photodiode. Therefore, the photocurrent was measured as a function of the VCSEL driving current and by taking into account the characteristics of the optoelectronic components, the total link loss was calculated. These measurements were performed before and after applying the index matching PDMS between the waveguide end-faces and optoelectronic components. In all experiments, VCSEL driving currents were applied using a Keithley 2401 Source Measure Unit (SMU) and the photocurrents were read

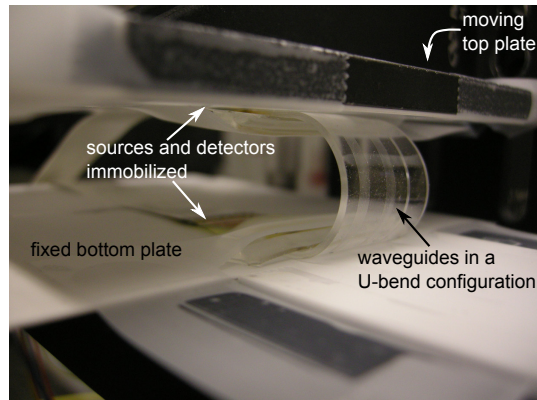


Fig. 6. Setup for investigating the effect of bending on the waveguide losses. The part of the sample where coupling between the optoelectronic components and the waveguides is performed was immobilized to exclude effects from changing coupling conditions as much as possible.

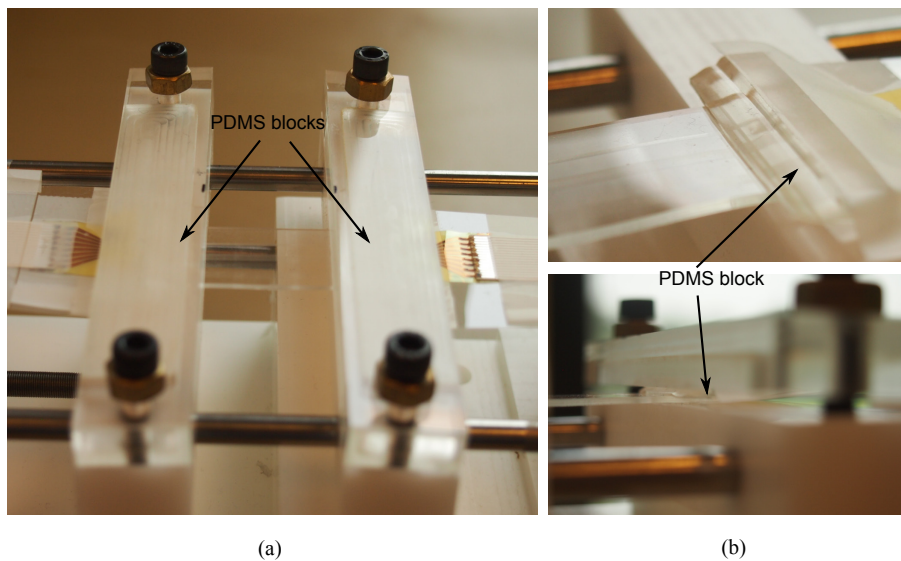


Fig. 7. Setup for investigating the effect of stretching on the waveguide losses: (a) the waveguide link mounted on the setup and (b) a close-up on the thicker PDMS protruding blocks attached on both sides allowing fixation without direct clamping on the waveguides themselves.

out using a second Keithley 2401 SMU at a fixed bias of -2 V. Both SMUs were interfaced using dedicated software to record the component characteristics.

The effect of bending on the waveguide losses was investigated using the setup shown in Fig. 6. The waveguide link including sources and detectors was attached to 2 plates positioning the waveguides in a U-bend. The bottom plate was kept fixed while the top plate was mounted on a motorized vertical stage. By moving the top plate, the waveguides were bent with radii from 11 mm down to 4 mm. The coupling region at the mirror plugs was immobilized to exclude effects from changing coupling conditions therefore only recording bending effects.

Then, the waveguides were subjected to mechanical stretching. In a first experiment, the waveguides were elongated for 30 % using a dedicated setup, see Fig. 7. The stretching mechanism consisted of a fixed and a moving holder positioned on guiding pins. Using a spindle, this moving holder was connected to a precision stepper motor, of which the direction of movement and speed was addressed by a commercial driving circuit, controlled by a programmable micro-controller unit. To limit the effect of changing coupling conditions, the waveguides were fixed away from the coupling region. Furthermore, a thicker block of PDMS was attached (using the ‘dry bonding’ technique explained above) on both sides of the waveguides to hold the sample without applying clamping pressure on the waveguides themselves, see Fig. 7.

Finally, the reliability of the waveguides during long term cyclic stretching was determined using an Instron 5543 advanced materials testing system. This way, the long term degradation or delamination of the waveguide stack could be tested. In this case, the sample was mounted vertically, but using a similar clamping system as in the previous experiment to relieve clamping stress on the waveguides. The VCSELs were driven by a fixed current (5 mA) during the complete experiment and the photodiodes were read out continuously during cyclic stretching. The test sample consisted of 3 parallel optical links on the same PDMS substrate, of which the middle 3 cm waveguide region was stretched for 80000 cycles at 10% elongation and a rate of 4 mm/s.

All bending and stretching experiments were performed on waveguide samples with index matching PDMS between the waveguide end-faces and optoelectronic components.

4. Results and discussion

4.1. Waveguide link loss

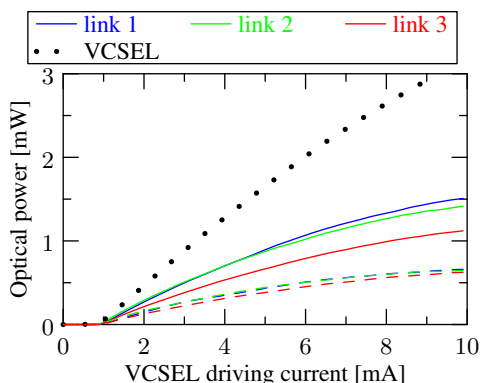


Fig. 8. Optical power detected by the photodiode, measured for 3 waveguide links. The dashed lines represent the case without, and the solid lines with index matching PDMS applied. The dotted curve represents the emitted VCSEL power.

After integrating the VCSELs and photodiodes with the waveguides, the optical power detected by the photodiode at the end of the optical link was recorded, and is plotted in Fig. 8 as a function of the applied VCSEL driving current. Based on the photodiode responsivity of 0.55 A/W, the recorded photocurrent was converted into optical power. The dashed lines in the graph represent the data before application of index matching PDMS material. In this case, the material between VCSEL, 45° deflecting mirror and waveguide end-face is air. The solid lines in the graph represent the data after application of index matching PDMS material (Sylgard®184) between the VCSEL, 45° deflecting mirror and waveguide end-face. As a comparison, also the

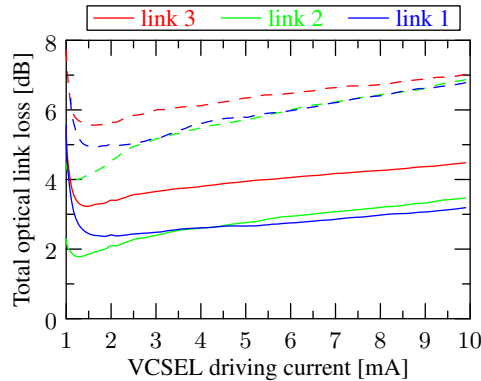


Fig. 9. Total optical loss in the waveguide link (in dB), measured for 3 waveguide links. The dashed lines represent the case without, and the solid lines with index matching PDMS applied.

intrinsic so-called LI characteristic of the VCSEL component is shown, i.e. its total emitted optical power as a function of driving current.

It is clear that application of the index matching PDMS significantly increases the amount of power detected by the photodiode. This can be explained by the lower divergence angle of the light beam in PDMS as compared to air, by the lower reflection losses and furthermore by the reduced influence of the waveguide end-face roughness on the coupling loss.

When determining the ratio of the VCSEL LI-characteristic and the power detected at the photodiode, the total optical link loss can be calculated. This result is represented on a dB-scale in Fig. 9 for the case with and the case without applied index matching PDMS. After application of this index matching material, total link losses between 2 and 4.5 dB were obtained, depending on the VCSEL driving current and the fabrication tolerances observed between different optical links. It can be observed that the link loss is generally lower for lower VCSEL driving currents owing to the smaller beam divergence angle of the VCSEL at lower driving currents so that light is coupled in the waveguide more efficiently. In previous work, the propagation losses of the PDMS waveguides were determined to be about 0.14 dB/cm, so that the waveguide propagation losses are estimated to be below 1 dB and the coupling losses between 0.5 and 1.75 dB per side.

4.2. Influence of waveguide bending

The effect of bending on the waveguide losses is displayed in Fig. 10 for 3 different optical links at 10 mA VCSEL driving current. The experiments were repeated for different VCSEL driving currents and similar results were obtained. Per link, the data of 3 identical experiments is plotted, and depicted using different line styles. Since the link loss of non-bended waveguides varies, the graph only shows the additional link loss as a function of bending radius of the waveguides, to allow an easier comparison between different waveguide links. It can be seen that bending has a negligible effect for bending radii down to 7 mm. For smaller values of the bending radius, the loss increases and this occurs not always in a monotonous fashion as would be expected. This may be explained by a slight local folding of the waveguide bend region during the experiment because of the rather thick (about 1 mm) but highly deformable PDMS waveguide substrate. The applied mechanical deformations may also slightly affect the coupling conditions at the interface with the optoelectronic components, which may contribute to seemingly random variations in the case of multimode systems.

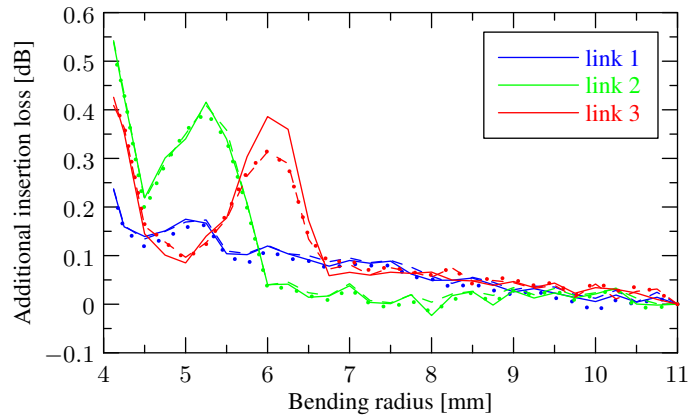


Fig. 10. Additional bending losses as a function of bending radius measured for 3 different waveguide links (depicted using different colors). The 3 separate experiments per link are depicted using different line styles (solid, dashed and dotted).

Due to the thickness of the PDMS blocks attached to the sample, it was not possible to measure bending radii smaller than 4 mm. However, it can be seen in Fig. 10 that the bending loss for two 90° bends becomes higher than 0.5dB (i.e. 0.25dB per 90° bend) when the bending radius becomes smaller than 4 mm. This corresponds with the results in [25], in which the bending losses of $50\ \mu\text{m} \times 50\ \mu\text{m}$ waveguides (with an NA of 0.25 and 1.14) were simulated using ray tracing simulations. It was found that the bending loss of a single 90° bend becomes higher than 0.25dB for bending radii between 3 and 9 mm, depending on the incoupling conditions and the numerical aperture of the simulated waveguide.

4.3. Influence of waveguide stretching

Figure 11 displays the additional optical losses recorded in 3 different links when stretching the waveguide region up to 30 % and subsequently releasing (9 cycles are shown in the graph). The driving current of the VCSEL obviously influences the amount of optical power received on the photodiode, but does not have a significant influence on differences in the relative loss expressed in dB. In all recorded cases, the extra loss due to stretching was limited to 0.7 dB, which is only a slight increase of the total link loss (see Fig. 9).

In all test cases, a periodic variation of the insertion loss was observed, but there were obvious differences between the links. Link 3 shows increasing insertion loss with elongation, whereas for link 1 and 2 this is not the case. This suggests that in addition to the stretching induced losses, also losses caused either by changing multimode conditions in the waveguide itself or by changing coupling conditions at the interfaces with the optoelectronic components are occurring. Although the sample was mounted on the setup so that the coupling conditions were kept as stable as possible, this effect can indeed not be completely excluded since mechanical stress during elongation can slightly influence the geometry of the coupling region. This is especially true since the waveguides are fabricated from a stretchable material. To minimize these loss fluctuations, the coupling region could be further stabilized using a local stiffener.

The waveguides can easily be stretched more than 30 %, but then it becomes difficult to maintain stability of the coupling region. Nevertheless, the waveguide substrate can be stretched up to 140 % before the PDMS material breaks.

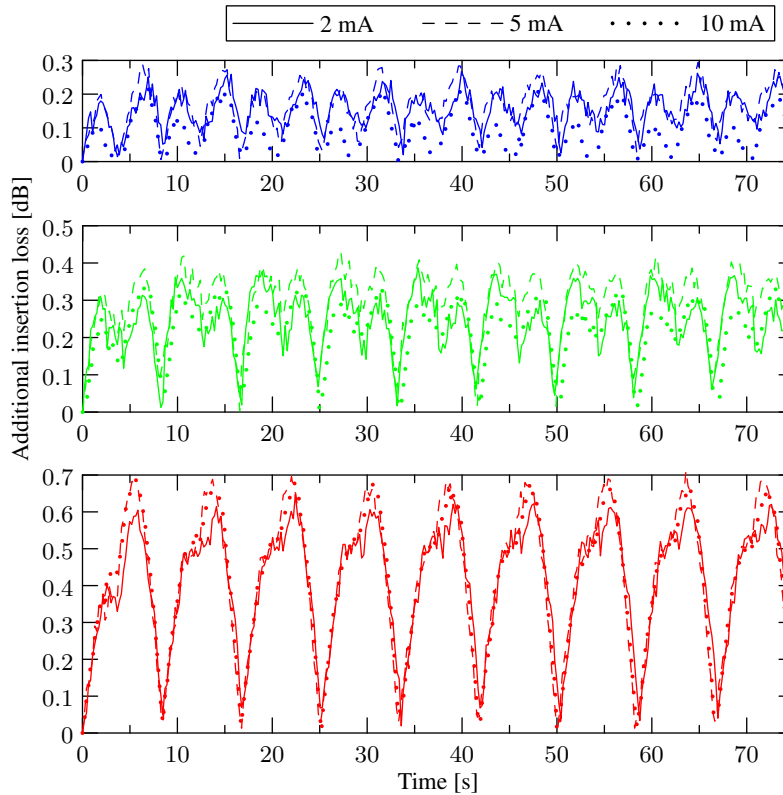


Fig. 11. Additional losses recorded when subjecting the waveguides to 9 cycles of 30 % elongation (8.3 s per cycle, waveguides unstretched at $t=0$ s). The experimental data for 3 different optical links is displayed in the 3 subplots showing link 1 to 3 from top to bottom. Within each subplot, the results for 3 different VCSEL driving currents are displayed using different line styles (solid, dashed and dotted).

4.4. Influence of long-term waveguide stretching

The results of the long-term stability testing of 3 optical links (on the same substrate) are shown in Fig. 12 (80000 cycles of stretching at 10 % elongation). In the graph, the insertion loss is shown after averaging over 50 cycles. This means that the variation during a single stretching cycle, as shown in Fig. 11, is not taken into account thereby only revealing influence of long-term aging effects providing an indication about the reliability of the complete optical link.

Although the loss variations during one cycle fluctuate between 0.2 and 0.7 dB, the long-term average insertion loss is very stable which indicates that the stretching does not introduce noticeable degradation. It can also be seen that the variations occur in a similar fashion for the different links, indicating possible effects of environmental influences. The test was eventually stopped at 80000 stretching cycles without a clear indication that degradation or failure would occur.

5. Conclusion

In this paper, the concept of stretchable optical waveguides was introduced. The technology for patterning these waveguides is based on a replication method, employing only commercially available PDMS materials. VCSELs ($\lambda = 850$ nm) and photodiodes embedded in a flexible

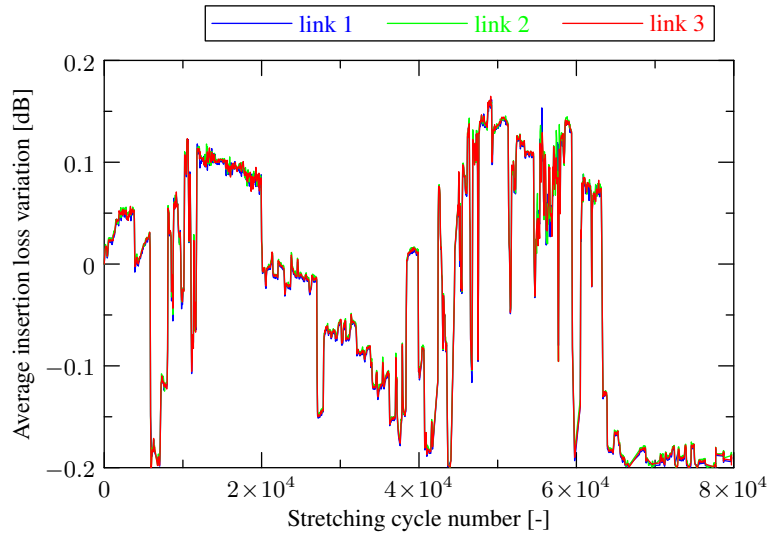


Fig. 12. Long-term optical link reliability testing: inter-cycle insertion loss variation of 3 optical links (data averaged over 50 cycles). These 3 optical links were present on the same substrate and therefore subjected to identical stretching conditions.

package were integrated with the waveguides resulting in a truly bendable, stretchable or mechanically deformable optical link. Furthermore, the integration of sources and detectors enabled the characterization of the total link loss and the influence of bending and stretching on the waveguide performance. A total link loss between 2 and 4.5 dB (this includes the coupling loss) was obtained for 6 cm long, $50\ \mu\text{m} \times 50\ \mu\text{m}$ PDMS waveguides. For bending radii down to 7 mm, only small extra losses were observed (maximum 0.1 dB) and during stretching up to 30 % elongation, the link remained functional and the observed extra loss was below 0.7 dB. However, it needs to be mentioned that during bending and stretching of the waveguide link, the effect of changing optical coupling conditions was observed at the interface with the optoelectronic components, which is inevitable due to the large mechanical deformability of the used PDMS materials. Finally, no clear degradation of the waveguide performance was observed after performing 80000 stretching cycles at 10 % elongation.